FISEVIER

Contents lists available at ScienceDirect

## Materials Science & Engineering A

journal homepage: www.elsevier.com/locate/msea



## Microstructure and anisotropic tensile behavior of laser additive manufactured TC21 titanium alloy



Qiang Zhang, Jing Chen\*, Zhuang Zhao, Hua Tan, Xin Lin, Weidong Huang

State Key Laboratory of Solidification Processing, Northwestern Polytechnical University, Xi'an, Shaanxi 710072, China

#### ARTICLE INFO

Article history: Received 9 March 2016 Accepted 9 July 2016 Available online 11 July 2016

Keywords: Laser additive manufacture Microstructure Anisotropic tensile behavior Titanium alloy

#### ABSTRACT

In the present work, two types of part with different geometries were fabricated by laser additive manufacturing (LAM) process under the same processing parameters. Tensile samples perpendicular to (horizontal) and parallel to (vertical) the build direction were produced after heat treated under different conditions. The results showed that the samples exhibit similar columnar  $\beta$  grains, but very different  $\alpha$  phase characterizations. The tensile properties show significant anisotropic. The sample containing finest  $\alpha$  laths shows highest ultimate tensile strength and yield strength. And the strength decreased with the increase of  $\alpha$  laths width. The total elongation of the samples does not show regularity relationship with the strength. The horizontal samples show inferior ductility and brittle fracture due to the columnar  $\beta$  grain morphology and the presence of continuous grain boundary  $\alpha$  layers. The coarse grain boundary  $\alpha$  layers after double heat treatment further reduced the ductility. The vertical samples exhibit better ductility due to lack of continuous grain boundary  $\alpha$  layers which perpendicular to the tensile load. The Vickers hardness test shows that the vertical samples were strengthened while the horizontal samples were little strengthened after tensile test.

© 2016 Elsevier B.V. All rights reserved.

#### 1. Introduction

Titanium alloys are widely used in the aeronautical industry for their high specific strength, excellent mechanical properties and outstanding corrosion resistance. However, the end products of titanium alloys are quite expensive due to the difficulties in refining, casting, forming and machining process [1]. Laser additive manufacturing is a kind of advanced processing technology that can be used to fabricate near fully-dense complex metal parts [2]. The LAM process has been recognized as an affordable and efficient solution that can meet the stringent requirements for aerospace titanium alloys components [3–5]. In order to achieve mechanical properties comparable or even superior to the traditional manufacturing, it is crucial to get a better and deeper understanding of the relationships between the processing parameters, microstructure evolution and the resulting mechanical properties.

During the LAM process, the deposited layers undergo melting, rapid solidification, partial remelting and reheating. Therefore, the LAM process resulted in a specific microstructure. It has been well documented that during solidification of the molten pool, the solid substrate acts as a heat sink and the as-deposited microstructure generally presents a directional solidified morphology grown from

the substrate epitaxially [6]. As a result, typical prior  $\beta$  grain morphology of LAMed  $\alpha + \beta$  titanium alloys usually comprised of coarsen columnar grains which exhibit a strong (100) fiber texture [7–9]. The characterization of  $\alpha$  phase precipitated in the  $\beta$  phase shows more complex features because the deposited layers experienced consecutive thermal cycles with a duration and amplitude which depend on the processing parameters and geometry of the part being fabricated [10]. Fine lamellar structure containing martensitic  $\alpha'$  [11], layer bands [12] and coarsen lamellar structure [13] have been reported. This specific microstructure characterization strongly effects the mechanical properties of LAMed titanium alloys. Generally, the LAMed titanium alloy components usually present anisotropic mechanical properties. The strongly textured prior  $\beta$  grains which growth along the build direction is regarded as the main reason for anisotropic mechanical properties [14–16]. Vilaro [17] found that the pores shape and orientation in the deposited Ti6Al4V components strongly influence the ductility. Qiu [18] found that the presence of planar pores due to incomplete remelting of previous layers in LAMed Ti6Al4V alloy also caused pronounced anisotropy in ductility. Carroll [4] studied the anisotropy tensile behavior in LAMed Ti6Al4V alloy cruciform component. They reported better ductility along the build direction in comparison to the direction perpendicular to the build direction. They believed that the columnar  $\beta$  grains and grain boundary  $\alpha$  phase are the main reason for different ductility.

The TC21 titanium alloy (Ti6Al2Sn2Zr3Mo1.5Cr2Nb,  $\beta$  transus

<sup>\*</sup> Corresponding author.

E-mail address: phd2003cjj@nwpu.edu.cn (J. Chen).

temperature is about 960 °C [19]) investigated in the present study is a  $\alpha+\beta$  titanium alloy. Due to the good balance of strength, ductility and fracture toughness, the TC21 titanium alloy has shown a good promising for applications in aerospace industry [20]. The previous study showed that the microstructure of LAMed TC21 titanium alloy is more inhomogeneous than the Ti6Al4V alloy due to the higher alloying elements [21]. Similar inhomogeneous microstructure could also been observed in other LAMed titanium alloys which contains more alloy elements [22,23]. However, there has been little effort to understand the connection between the mechanical properties and the more complex microstructure characterization. The aim of this study is to correlate the microstructure of LAMed TC21 titanium alloy to the corresponding tensile properties. In the present work, two types of part with different geometries were deposited under the same LAM processing condition. And then the tensile properties parallel to and perpendicular to the build direction after two different heat treatments were tested. Based on the experiment results, the anisotropic tensile behavior and the relationship with the microstructure characterization were discussed.

#### 2. Experimental procedures

The samples were fabricated by a LAM equipment that consists of a 4 kW continuous wave CO<sub>2</sub> laser, a 5-axis numerical control working table, a coaxial powder feeder nozzle and an inert gas chamber filled with pure argon with oxygen content below 50 ppm. TC21 spherical powders produced by the plasma rotating electrode process (PREP) were used as the deposited material. The powder size ranges from 80  $\mu m$  to 150  $\mu m$ . The powders were dried in a vacuum oven for 2 h at 120  $\pm$  5 °C to eliminate the moisture absorption and ensure the powders have good flow ability. The forged TC21 plates were used as substrate for the LAM process. The depositing surface was sanded with SiC paper and then degreased with acetone and ethanol.

A cross-hatching scanning strategy was used in this study. Two types of part with different geometries were deposited in order to evaluate the tensile properties that parallel to and perpendicular to the build direction. The scanning strategy and part geometries are illustrated in Fig. 1. All the samples were deposited under the same processing condition (Laser power: 2000 W, scanning velocity: 10 mm/s, powder feed rate: 8 g/min, norminal increment of Z axis: 0.4 mm, overlap rate: 40%). The deposited samples were divided into two batches: the first one was subjected to ageing treatment (600 °C, 2 h/AC). The second one was subjected to double treatment (solution and ageing, 870 °C, 1 h/FC+600 °C,

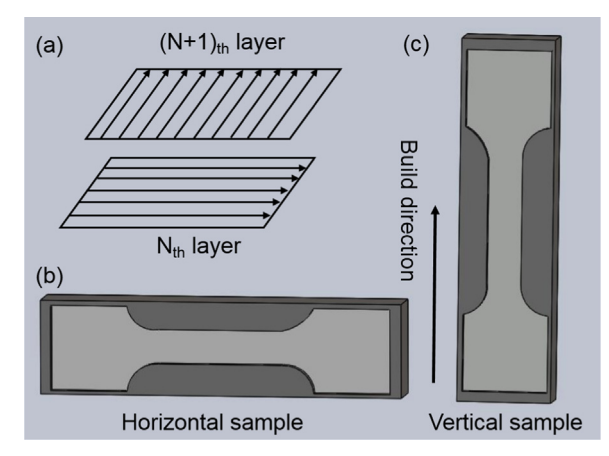


**Fig. 1.** (a) cross-hatching scanning strategy, (b) horizontal sample, (c) vertical sample.

**Table 1**The nomenclature and detail information of the tensile samples.

Sample	Tensile direction	Heat treatment
H-AT V-AT H-DT	Horizontal Vertical Horizontal	600 °C, 2 h/AC 870 °C, 1 h/FC+600 °C, 2 h/AC
V-DT	Vertical	

2 h/AC). After heat treatment, the tensile samples (6.0 mm in gauge width, 2 mm in gauge thickness and 30 mm in gauge length) were machined by electrical discharge machining and then sanded with SiC paper. The nomenclature and detail information of the tensile samples was listed in Table 1. All the samples were subjected to room temperature tensile testing at a constant crosshead displacement rate of 1 mm/min on an Instron-3382 testing machine.

Strain evolution of the sample was investigated by using an optical system incorporated with digital image correlation system (DIC). All the samples were prepared with spray-painted black speckles on a white paint layer providing a random speckle pattern for the DIC system to follow. During the tensile test, the deformation was recorded by the DIC system and then the taken images were analyzed with the help of an in-house software.

Microstructure of the gauge section was investigated by optical microscopy (OM, Keyence VH-Z50L) and scanning electron microscopy (SEM, Tescan VEGAIILMH). Kroll reagent (1 ml HF, 3 ml HNO<sub>3</sub> and 50 ml H<sub>2</sub>O) was used to reveal the microstructure of all the samples after mounting, grinding and polishing. Vickers hardness before and after tensile test were measured at 1 mm intervals at the gauge section using a micro Vickers hardness meter (Struers Duramin-A300). The Vickers hardness tests were performed by applying a load of 9.8 N for 15 s. Vickers hardness and microstructure investigation before tensile test was performed on the samples taken from the same position where the corresponding tensile sample was cut out.

#### 3. Results

#### 3.1. Microstructure

Macrostructure and microstructure of the horizontal samples are presented in Fig. 2. Columnar prior  $\beta$  grains which extend over multiple layers can be observed in Fig. 2a and c. According to the previous studies, the columnar prior  $\beta$  grains present a strong  $\langle 100 \rangle$  fiber texture [21]. As distinct from the prior  $\beta$  grain morphology, the  $\alpha$  phase characterization is quite different. The sample H-AT exhibits a dense distribution of very fine  $\alpha$  laths within the  $\beta$  grains (Fig. 2b). The width of  $\alpha$  laths is about 0.14  $\mu$ m. Very thin grain boundary  $\alpha$  layer ( $\alpha_{GB}$ ) can also be observed. Besides, the molten pool boundaries can be observed clearly in sample H-AT. The molten pool boundaries exhibit a regular structure. Coarse  $\alpha$  laths with smaller aspect ratio can be observed in sample H-DT (Fig. 2d). The width of  $\alpha$  laths in sample H-DT is about 1  $\mu$ m. Both continuous and discontinuous  $\alpha_{\text{GB}}$  layers can be observed in the horizontal samples. The width of  $\alpha_{GB}$  layer is about 4  $\mu m$ . As indicated by the black arrows in Fig. 2c, much thicker  $\alpha_{GB}$  layers can also be observed at  $\beta$  grain boundaries. In general, the morphology and scale of the precipitated  $\alpha$  laths are relative uniform in the two horizontal samples.

As shown in Fig. 3a and c, similar columnar prior  $\beta$  grains can be observed in the vertical samples. Layer bands structure can be observed clearly in the pictures. As shown in Fig. 3b, layer bands in sample V-AT consist of fine  $\alpha$  laths. The width of  $\alpha$  laths in the

### Download English Version:

# https://daneshyari.com/en/article/1573128

Download Persian Version:

https://daneshyari.com/article/1573128

<u>Daneshyari.com</u>